A Maximum Constant Boost Quasi-Z-Source Invertor with Third Harmonic Injection for Linear Induction Motors

Vignesh Radhkrishnan
AUT University
31-33 Symonds Street
Auckland, NEW ZEALAND

Shubhendu Baghel
AUT University
31-33 Symonds Street
Auckland, NEW ZEALAND

Adam PR Taylor
AUT University
31-33 Symonds Street
Auckland, NEW ZEALAND

Abstract- **Three phase voltage linear induction motors (LIMs) are emerging as a reliable means of providing both fast transport solutions and significant amount of linear thrust. However, conventional Voltage Source Invertor (VSI) and Current Source Invertor (CSI) motor drives applied to LIMs suffer from the generation of harmonic currents from the nonlinear nature of the LIM. This paper presents an improved Quasi-Z-Source Inverter (QZSI) for a linear induction motor (LIM) whose controller has been built, and its simulated results. The proposed QZSI controller herein for a LIM will injects uniformly spaced shoot through states, and promises a high output voltage gain and reduced THD.**

I. INTRODUCTION

Linear Induction Motors (LIMs) are coming to the fore as a means of providing significant linear thrust capable of launching aeroplanes [1] and as the driving technology behind mass transport systems [2]. The two most common types of speed drives used to drive the LIM are the voltage source inverter (VSI) [3] and current source inverter (CSI) [4]. However, the VSI is limited in that the output voltage cannot exceed the input voltage without additional expensive circuitry, which in turn lowers the overall system efficiency. Similarly, the CSI cannot be used as buck inverter as it is also expensive and the degradation of line-side power factor must be corrected.

The proposed Quasi-Z-Source Invertor (QZSI) [5] offers a wide voltage gain and draws a constant current from the source and can act as a buck/boost convertor [6], unlike the VSI and CSI, as the impedance network incorporated in between the source and the bridge circuit permits the simultaneous conduction of the switching devices in the same leg.

II. BACKGROUND

Linear Induction Motors (LIMs)

A LIM employs a poly-phase AC supply connected to a 'primary' made of windings wound around poles made of laminated steel (Fig. 1), and it has been suggested that chamfering the edges of the primary will improve performance [7].
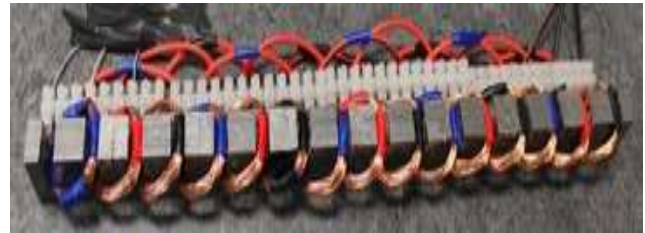

Fig. 1. An example of a LIM primary stator, showing polyphase windings around laminated steel

The 'secondary' reaction plate shown in Fig. 2 is typically made from mild steel, aluminium, copper or a combination of these materials to obtain desired combination of their features, and an air gap (g_m) separates the secondary reaction plate from the laminated windings, as shown in Fig. 2. A travelling magnetic wave is established in the primary from the poly-phase supply, which is induced into the secondary and creates a second magnetic field. The reaction between these two magnetic fields generates (linear) thrust.
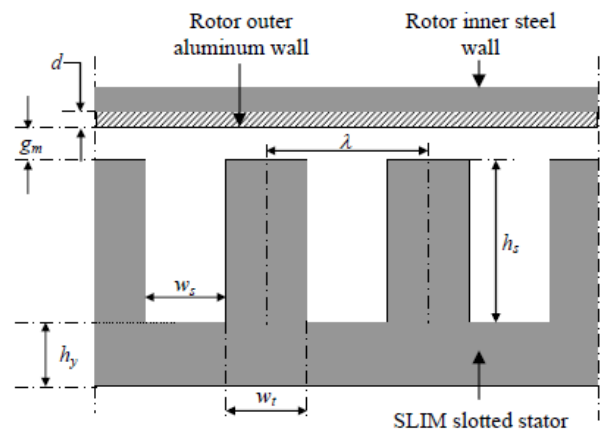

Fig. 2. LIM geometry [8]

The force generated, F_m, is a function of developed power (P_r) over relative speed (V_r), or air gap power (P_g) over synchronous speed (V_s), or reaction plate current (I_2), resistance in the secondary (r_2) and slip (s), and is summarised in Eqn.(1).

$$F_m = \frac{P_r}{V_r} = \frac{P_g}{V_s} = 3I_2^2\left(\frac{r_2}{s}\right) \quad (1)$$

232

An equivalent circuit of each phase of a LIM is given in Fig. 3, below. Core losses can be neglected because the airgap flux density leads to medium flux densities in the core and therefore a rather low core loss [9]. A LIM with a thin conductive sheet on the secondary will have minimal skin effect and therefore equivalent rotor inductance can be ignored [9].
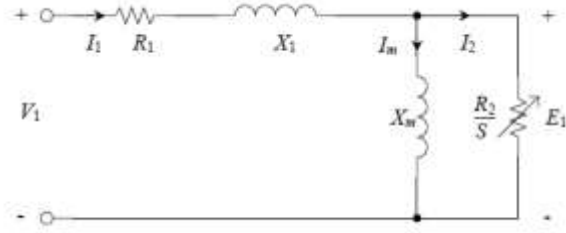

Fig. 3. A per-phase equivalent circuit of the LIM

The resistance of each phase of the LIM stator winding R_1 is calculated by:

$$R_1 = \rho_w \frac{l_w}{A_{wt}} \qquad (2)$$

where ρ_w is the copper wires volume resistivity used in stator winding, l_w is the length of the copper wire per phase and A_{wt} is the cross sectional area of the wire.

The flux produced in the stator windings is reduced due to flux leakage in the stator slots, X_1, as shown in Eqn.(3), and is caused by the slot openings of the stator core [9]. In a LIM with open rectangular slots and double layer windings, X_1, is found by:

$$X_1 = \frac{2\mu_0 \pi f[(\lambda_s(1+\frac{3}{p})+\lambda_d)\frac{W_S}{q_1}+\lambda_e l_{ce}]N_1^2}{p} \quad (3)$$

Where

$$\lambda_s = \frac{h_s(1+3k_p)}{12 w_s} \qquad (4)$$

k_p is the pitch factor, and

$$\lambda_e = 0.3(3k_p - 1) \qquad (5)$$

And

$$\lambda_d = \frac{5(\frac{g_e}{w_s})}{5+4(\frac{g_0}{w_s})} \qquad (6)$$

The per-phase magnetizing reactance X_m shown in Fig. 3 can be given by this calculation:

$$X_m = \frac{24\mu_0 \pi f W_{se} k_w N_1^2 \tau}{\pi^2 p g_e} \qquad (7)$$

Where g_e is the equivalent air gap given in Eqn.(3), k_W is the winding factor given in Fig. 3 and W_{se} is the equivalent stator width calculated by:

$$W_{se} = W_s + g_0 \qquad (8)$$

The per phase rotor resistance R_2 is a function of the slip, and R_2 can be determined from the goodness factor, G, and the per phase magnetizing reactance X_m, below

$$R_2 = \frac{X_m}{G} \qquad (9)$$

We can define the goodness factor from;

$$G = \frac{2\mu_0 f \tau^2}{\pi(\frac{\rho_r}{d})g_e} \qquad (10)$$

The magnitude of the rotor phase current can be calculated from;

$$I_2 = \frac{X_m}{\sqrt{(\frac{R_2}{S})^2 + X_m^2}} I_1 \qquad (11)$$

And the magnetizing current can be found through:

$$I_m = \frac{I_1 R_2}{\sqrt{R_2^2 + (S X_m)^2}} \qquad (12)$$

The final calculation is the total circuit impedance which is can be calculated from this equation:

$$Z = R_1 + jX_1 + \frac{j(\frac{R_2}{S}X_m)}{\frac{R_2}{S}+jX_m} \qquad (13)$$

The Impedance (Z) Source Inverter (ZSI)

The Impedance (Z) Source Inverter (ZSI) [10, 11] contains an impedance network consisting of two inductors and two capacitors on the front end of a three phase invertor, as shown in Fig. 4, below.
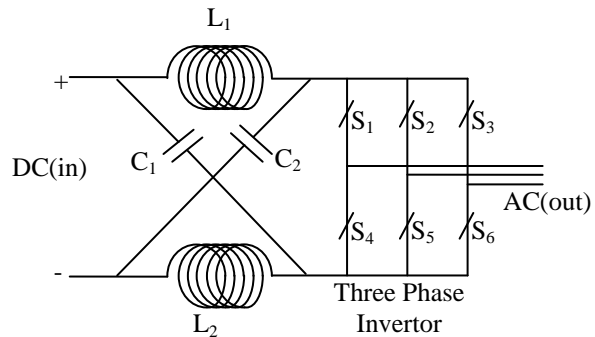

Fig. 4. Z-Source Invertor Topology

Switches S_1-S_6 provide bidirectional current flow and unidirectional voltage blocking. Inductors L_1-L_2 need to be large to minimise ripple, or even discontinuous, currents and are connected in series with the three phase invertor and capacitors C_1-C_2 are connected diagonally across L_1-L_2. The L-C network establishes buck or boost capability, subject to the boosting factor and acts as a second order filter. Switching of switches S_1-S_6 can be in the conventional 'non-shoot-through state' that incorporates dead-time to prevent a short of the DC rail if S_1 and S_4, or S_2 and S_5, or S_3 and S_6 are both on. Alternatively switching that utilises the shoot-through state to boost the DC voltage available to the three phase invertor, whereby S_1 and S_4, or S_2 and S_5, or S_3 and S_6 are both on can be used due to the presence of the L-C network.

III. THE QUASI-Z-SOURCE INVERTER

The Quasi-Z-Source Inverter (QZSI) [12] is a single stage power converter derived from the Z-source inverter topology shown in Fig. 4. However, the QZSI employs a unique impedance network as shown in Fig. 5, below, that allows several shoot-through zero states to be produced.
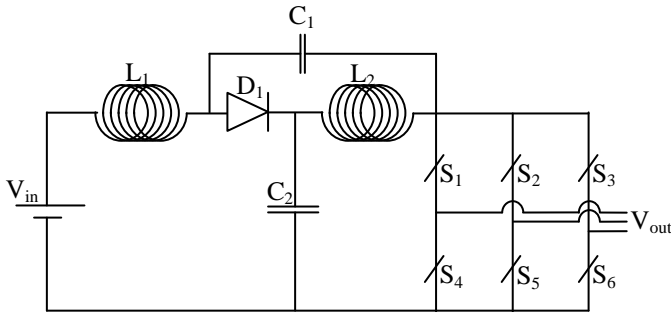

Fig. 5. The Quasi-Z-Source Invertor

The unique impedance network enables the inverter to boost the voltage whilst drawing a constant current over a wide input voltage range due to L_1. Given the positioning of L_1, L_2, C_1, and C_2 in the QZSI, these devices are exposed to the full brunt of V_{in} and therefore are a key deign consideration. The QZSI facilitates lower component ratings, switching ripple, and supply stress that the ZSI [10, 13], and as a continuous input current topology with both a non-zero and low inrush input current there is significantly reduced stress to the input voltage source.

The QZSI has several operational states: the six conventional active states of a three phase H-Bridge Invertor; two zero states, where either S_1 and S_2 and S_3, or S_4 and S_5 and S_6 are on; and three shoot-through states, where S_1 and S_4, or S_2 and S_5, or S_3 and S_6 are on. Each of these states delivers the supply through the switches and the passive components, and energy from the supply gets stored in these passive components and then delivered into the load in a non-shoot-through state.

The shoot-through capability increases reliability [14] along with a low common-mode noise profile [15]. A low-pass filter may be installed on the output of the QZSI. During the shoot-through states, the DC link voltage depends on the shoot through duty ratio for a given modulation index, and the uniformly spaced shoot through states provide for a reduced THD, and with no ripple a [16].

The QZSI in Non-Shoot-Through Mode

When operating in non-shoot-through mode, the QZSI operates as a conventional voltage source invertor and the inverter bridge can be considered as a current source. Therefore, in the non-shoot-through mode:

$$V_{L1} = V_{in} \tag{14}$$

$$V_{L2} = -V_{C2} \tag{15}$$

$$V_{PN} = 0 \tag{16}$$

$$V_{D1} = V_{C1} + V_{C2} \tag{17}$$

where V_{PN} is the voltage applied to the switches.

The QZSI in Shoot-Through Mode

When operating in shoot-through mode, the QZSI can turn on S_1 and S_4, or S_2 and S_5, or S_3 and S_6 both on for a very short duration without delivering a short to the supply voltage due to the presence of the L-C network while simultaneously increasing the output voltage by a ratio (D) of the shoot-through time (T_0) to the non-shoot-through time (T_1), as shown in Eqn.(18), below.

$$D = \frac{T_0}{T_1} \tag{18}$$

During the shoot-through state, the inductor current increases linearly and the voltage across the inductor is equal to the voltage across the capacitor [17]. T_0, the diode D_1 is open circuit and therefore;

$$V_{L1} = V_{C2} + V_{in} \tag{19}$$

$$V_{L2} = V_{C1} \tag{20}$$

$$V_{PN} = 0 \tag{21}$$

$$V_{D1} = V_{C1} + V_{C2} \tag{22}$$

Rearranging the above yields

$$V_{L1} = \frac{T_0(V_{C2} + V_{in}) + T_1(V_{in} - V_{C1})}{T} \tag{23}$$

$$V_{L2} = \frac{T_0 V_{C1} - T_1 V_{C2}}{T} \tag{24}$$

IV. QZSI DESIGN FOR A LINEAR INDUCTION MOTOR

Switching Design

For simple boost control of the QZSI, the shoot through duty ratio is inversely proportional to, and limited by, the modulation index as shown in Eqn.(25), below.

$$D_s = 1 - m_a \qquad (25)$$

where m_a is modulation index indicating the total active states per period. The boost factor, B, of simple boost control equals to;

$$B = \frac{1}{1 - 2D_s} = \frac{1}{2m_a - 1} \qquad (26)$$

And the gain, G, using simple boost control can be seen in Eqn.(27), below,

$$G = \frac{2V_{AC}}{V_{DC}} = m_a B = \frac{B+1}{2} \qquad (27)$$

where V_{AC} is the peak value of inverter output phase voltage and V_{DC} is the average DC-link voltage. The voltage stress, Vs, can be found by Eqn,(28), below.

$$V_S = 2GV_{in} \qquad (28)$$

Eqn.(25), Eqn.(26), Eqn.(27), and Eqn.(28) suggest that to a high gain requires a small modulation index, and therefore higher voltage stress on the switching devices will occur.

Maximum constant boost control can be obtained by maintaining a constant shoot-through duty ratio, resulting in the eliminations of low frequency ripple will be eliminated in the QZSI. This is achieved by comparing the upper and the lower shoot-through values and the frequency should be three times higher than the output frequency [12, 18].

Reduction in the total harmonic distortion can be achieved with the injection of the third harmonic into the reference sine wave [19], and is considered optimum.

The Linear Induction Motor (LIM) to be controlled by the QZSI could draw 43A when supplied with 150V. Knowing the maximum gain, G_{max}, Eqn.(29),

$$G_{max} = \frac{V_{AC}}{\left(V_{in}/2 \right)} \qquad (29)$$

$$M_{min} = \frac{G_{max}}{\left(\sqrt{3}G_{max} \right) - 1} \qquad (30)$$

$$D_{max} = 1 - \frac{\left(\sqrt{3}M \right)}{2} = 0.227 \qquad (31)$$

$$T_{0\,max} = \frac{2 - \left(\sqrt{3}M_{min} \right)}{f_s} = 28\mu S \qquad (32)$$

With a boundary ripple current of 20% in the inductors, the inductor L_1 and L_2 values are found through Eqn.(33), below, to be 213μH

$$L = \frac{MV_{in}T_{0_{max}}}{2I_{in}C} = 213\mu H \qquad (33)$$

With a voltage ripple boundary condition of 1% on the capacitors C_1 and C_2, are found to be 182μF.

$$C = \frac{2I_{in}T_{0_{max}}}{2BV_{in}T_v} = 182\mu F \qquad (34)$$

V. QUASI-Z-SOURCE INVERTOR SIMULATION AND BUILD

The QZSI was simulated to verify the proposed control strategies contained herein, and the controller built on a FPGA platform for the Linear Induction Motor (LIM). The simulation results were consistent with the theoretical analysis, which verifies the control concept. With the same input voltage and the same required output voltage, the maximum constant boost control with third harmonic injection achieve much lower voltage stress across the devices than the simple boost control.

The maximum constant boost control employed is shown in Fig. 6, with the switching waveforms shown in Fig. 7, below.
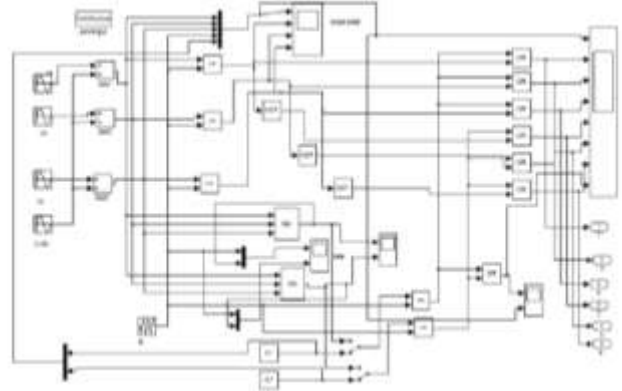

Fig. 6. Maximum Constant Boost Control Topology

Fig. 7. Maximum Constant Boost Control Switching Waveforms

The output waveforms from start-up are shown in Fig. 8, below, and show a stabilisation with four cycles, or 80mS.
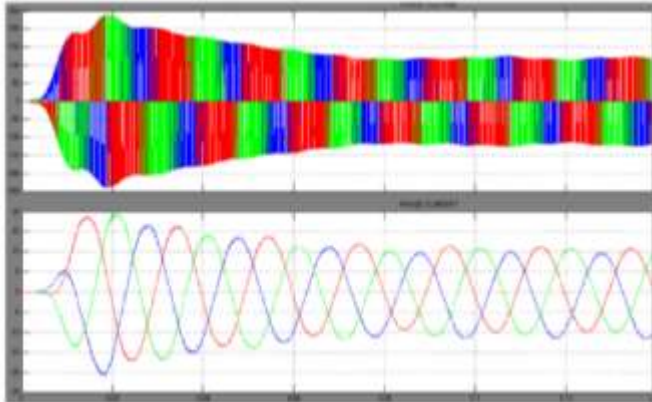

Fig. 8.   QZSI Voltage (top) and Current (bottom) Output Waveforms

The controller board was built on a Spartan 6 FPGA controller using 6N137 opto-couplers working into IR2110 high and low side MOSFET/IGBT drivers, and is shown in Fig. 9, below.

Fig. 9.   Completed Controller Board for the Quasi-Z-Source Invertor

VI.   CONCLUSION

A Quasi-Z-Source Invertor (QZSI) controller for a Linear Induction Motor (LIM) has been designed, simulated, verified, and built. The FPGA controlled QZSI injects uniformly spaced shoot through states that delivers a high output voltage gain and a reduced THD. The controller employs a novel control strategy that utilises maximum constant boost along with the injection of the third harmonic to address the inherent non-linearities of a LIM.   Consequently the QZSI with maximum constant boost and third harmonic injection provides a higher voltage gain and reduced harmonics and IGBT stresses in driving the LIM.

REFERENCES

[1]   S. Mu, J. Chai, X. Sun, S. Wang, "A novel linear induction motor for electromagnetic aircraft launch system" 2014 17th International Symposium on Electromagnetic Launch Technology (EML), La Jolla, CA, 7-11 July 2014

[2]   R. Zhang, Y. Du, Y. Li, K. Wang, H. Qiu, "Experimental research of linear induction motor for urban mass transit" 2010 International Conference on Electrical Machines and Systems (ICEMS), Incheon, 10-13 Oct. 2010

[3]   K.S. Rajashekara, V. Rajagopalan, A. Sevigny, and J. Vithayathil,"DC link filter design considerations in three-phase voltage source inverter-fed induction motor drive system" Industry Applications, IEEE Transactions on, IA-23(4):673–680, July 1987.

[4]   Q. Lei, F.Z. Peng, and B. Ge, "Transient modeling of current-fed quasi-z-source inverter" In Energy Conversion Congress and Exposition (ECCE), 2011 IEEE, pages 2283–2287, Sept 2011.

[5]   M.A. Ismeil, A. Kouzou, R. Kennel, H. Abu-Rub, and M. Orabi, "A new switched-inductor quasi-z-source inverter topology" In Power Electronics and Motion Control Conference (EPE/PEMC), 2012 15th International, pages DS3d.2– 1–DS3d.2–6, Sept 2012.

[6]   Y. Li, J. Anderson, F.Z. Peng, and D. Liu. "Quasi-z-source inverter for photovoltaic power generation systems" In Applied Power Electronics Conference and Exposition, 2009. APEC 2009. Twenty-Fourth Annual IEEE, pages 918–924, Feb 2009.

[7]   H-W. Lee, C-B. Park, B-S. Lee. "Thrust Performance Improvements of a Linear Induction Motor", Journal of Electrical Engineering & Technology", vol.6, No.1, pp. 81-85, 2011

[8]   S. P. Bhamidi, (2005). "Design of a single sided linear induction motor" Missouri

[9]   R. Pai, I. Boldea, and S. Nasar, "A complete equivalent circuit of a linear induction motor with sheet secondary" Magnetics, IEEE Transactions on , pp. 639 – 654, 1998

[10]   S. Yang, F. Peng, Q. Lei, R. Inoshita, and Z. Qian, "Current-fed quasi-z-source inverter with voltage buck-boost and regeneration capability" In Energy Conversion Congress and Exposition, 2009. ECCE 2009. IEEE, pages 3675–3682, Sept 2009.

[11]   D. Cao, S. Jiang, X. Yu, and F. Z. Peng, "Low-cost semi-z-source inverter for single-phase photovoltaic systems" Power Electronics, IEEE Transactions on, 26(12):3514– 3523, Dec 2011.

[12]   Y. Ding, L. Li, and J. Liu. "High frequency transformer isolated cascaded quasi-z-source inverter" In Industrial Electronics and Applications (ICIEA), 2012 7th IEEE Conference on, pages 792–796, July 2012.

[13]   S. Sonar and T. Maity. "Wind power conversion based on quasi-z source inverter" In Control, Automation, Robotics and Embedded Systems (CARE), 2013 International Conference on, pages 1–6, Dec 2013.

[14]   A. Battiston, El-Hadj Miliani, S. Pierfederici, and F. Meibody-Tabar. "A novel quasi-z-source inverter topology with special coupled inductors for input current ripples cancellation" Power Electronics, IEEE Transactions on, pp(99):1–1, 2015.

[15] Q. Lei, D. Cao, and F. Z. Peng. "Novel loss and harmonic minimized vector modulation for a current-fed quasi-z-source inverter in HEV motor drive application" Power Electronics, IEEE Transactions on, 29(3):1344–1357, March 2014.

[16] F. Z. Peng, A. Joseph, J. Wang, M. Shen, L. Chen, Z. Pan, E. Ortiz-Rivera, and Yi Huang. "Z Source inverter for motor drives" Power Electronics, IEEE Transactions on, 20(4):857–863, July 2005.

[17] E. Afjei B. Anvari, M. Shirinabadi. "Design and simulation of z-source inverter for brushless dc motor drive" In International Research Journal of Applied and Basic Sciences, pages 417–421, 2013.

[18] C.J. Gajanayake, H.B. Gooi, F.L. Luo, P.L. So, L.K. Siow, and Q.N. Vo. "Simple modulation and control method for new extended boost quasi z-source" In TENCON 2009 - 2009 IEEE Region 10 Conference, pages 1–6, Jan 2009.

[19] H. Latifi and W. Hosny. "Novel control technique for quasi z-source with improved voltage gain and reduced THD" In Electrical Engineering (ICEE), 2014 22nd Iranian Conference on, pages 545–549, May 2014.